

Response of fibre reinforced aluminium–lithium laminates to different fatigue conditions

S. B. DAVENPORT*, P. J. GREGSON

Department of Engineering Materials, University of Southampton, Southampton, UK

R. MORETON, C. J. PEEL

Structural Materials Centre, DRA, Farnborough, UK

Under fatigue conditions fibre reinforced aluminium–lithium laminates do not respond in the same manner as monolithic aluminium alloys. The variation of fatigue crack growth rates with initial loading condition has been examined for both carbon and glass fibre reinforced laminates, and compared with the behaviour of unreinforced 8090 aluminium–lithium alloy for a range of conditions (different initial nominal stress intensity factor range, load range and reversed loading). During fatigue, cracks grow in the metal layers of these laminates whilst the fibres in the crack wake remain intact, bridging the crack faces. The fibre bridging mechanism, inherent in this laminate system, reduces the fatigue crack growth rate. The magnitude of the bridging effect appears to be inversely related to the applied load range. This relationship can account for the behaviour observed in the performed experiments.

1. Introduction

Fibre reinforced aluminium–lithium laminates are a lightweight hybrid composite intended to replace monolithic Al-alloys in fatigue critical areas of aircraft structures. Under dynamic loading conditions the laminates generally exhibit considerably lower crack growth rates than the unreinforced alloy they are replacing. This is because of a “fibre bridging” mechanism which occurs within the material, where the fibres in the wake of the fatigue crack remain intact and act so as to reduce crack growth rates [1]. However these laminates do not respond in the same manner as monolithic alloys to changing load conditions. The present research relates the mechanism of fatigue crack growth in the laminates to their observed response to different initial loading conditions.

2. Experimental procedures

The laminates comprised a 2-1 lay-up, that is a single layer of fibre reinforced epoxy resin sandwiched between two layers of aluminium–lithium alloy, 8090. The metal layers were cold-rolled to the appropriate gauge (0.45 mm), flattened by a 2% stretch and aged for 42 h at 170 °C, following this all the sheets were etched and anodized in chromic acid to improve the bond quality. The laminate was laid up using pre-pregs of XAS carbon fibres in Fibredux 913 (though these were later replaced with TS fibres) or E-glass fibres in Fibredux 913 laid unidirectionally, these were

cured in an autoclave at 120 °C for 2 h. Laminates were tested in the as-cured condition. Monolithic 8090 sheets were also cold rolled to the same overall thickness as the laminates and were heat treated in the same manner.

Fatigue panels were guillotined to the correct dimensions, 350 × 152 mm, and were tested in the centre cracked tension (CCT) specimen configuration with loads applied parallel to the fibre orientation. Cracks initiated from a through thickness slot cut in the centre of the panel in a lateral direction. Each panel was identified and described according to a numbering system, e.g., 8C3/4: “8” denotes the use of Al-alloy 8090, “C” – carbon fibre reinforcement (G – glass fibres and M – monolithic alloy), “3” – the number of layers in the panel, and “4” – that this was the fourth panel tested.

The tests were carried out in a Mand 250 kN servo-hydraulic test machine controlled by a Dartec digital control system. The crack length was monitored using a 4-probe pulsed potential drop (p.d.) system. The p.d. reading was plotted on a $x-t$ plotter, and was used to calculate both the crack growth rate (da/dN , where a = half the total crack length and N = the number of load cycles applied) and the nominal stress intensity factor range (ΔK).

Post-test analysis was carried out using the following techniques:

(i) Alloy layers were removed by chemical digestion in a bath of concentrated sodium hydroxide. The

* Present address: Department of Mechanical Engineering, University of Sheffield, Sheffield, S1 3JD, UK.

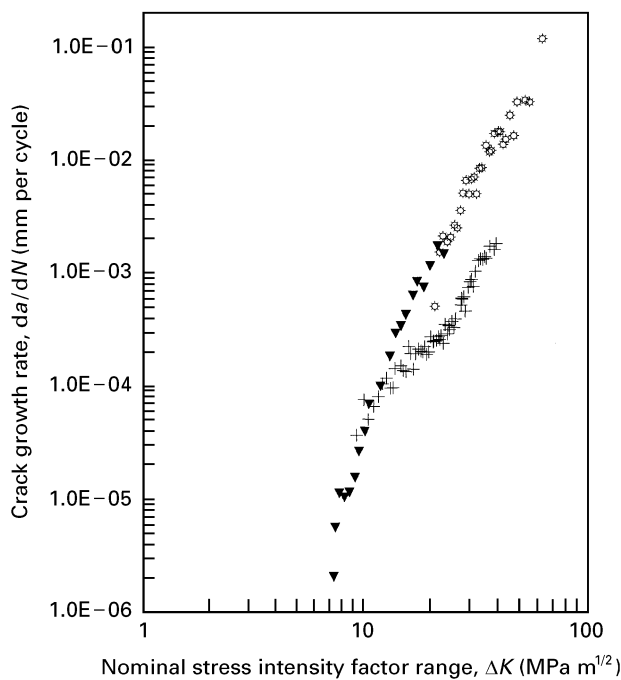


Figure 1 Response of glass fibre reinforced laminates to different initial ΔK values. Key: (+) 8G3/1; $\Delta K = 9.82 \text{ MPa m}^{1/2}$, (\odot) 8G3/2; $\Delta K = 16.00 \text{ MPa m}^{1/2}$ and (\blacktriangledown) 8M1/5; $\Delta K = 8.0 \text{ MPa m}^{1/2}$.

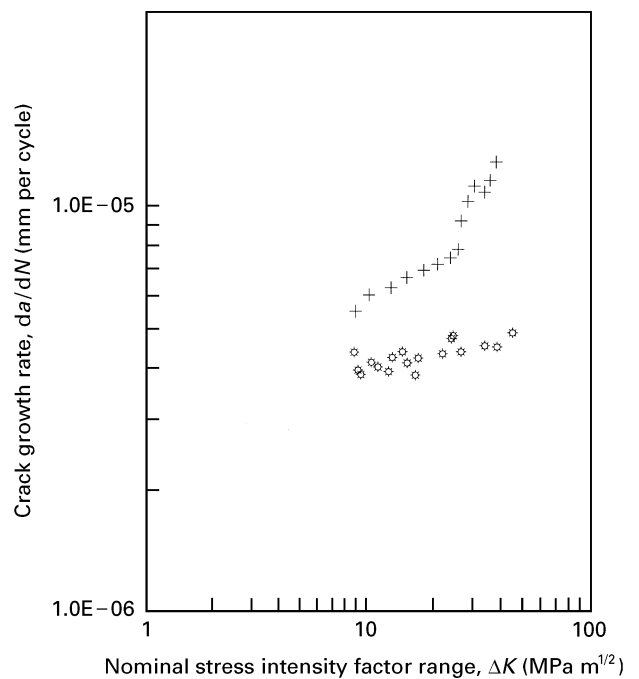


Figure 2 Response of carbon fibre reinforced laminates to comparable initial ΔK values. Key: (+) 8C3/12; $2s = 8.8 \text{ mm}$, $\Delta K = 8.36 \text{ MPa m}^{1/2}$, (\odot) 8C3/9; $2s = 10.00 \text{ mm}$, $\Delta K = 8.64 \text{ MPa m}^{1/2}$.

revealed composite ply was then examined in a scanning electron microscope (SEM).

(ii) Serial sections were taken along the length of the fatigue cracks. These were vacuum impregnated using an epoxy resin containing a fluorescent dye. Sections were then ground and polished until suitable for optical microscopy, which was carried out using the Nomarski differential interference technique.

(iii) Fatigued laminates were ultrasonically C-scanned.

(iv) The fracture surface of fatigue cracks from the metal layers were examined in the SEM.

3. Results

Fatigue tests were carried out on carbon and glass reinforced laminates to assess the effect of varying the initial ΔK (ΔK_i), since this is the basic parameter which describes crack growth in metals. Testing at different ΔK_i (Figs 1 and 2), or even the same ΔK_i (Fig. 3), resulted in non-co-linear curves for each condition. This behaviour is not characteristic of monolithic aluminium alloys.

ΔK_i is a function of the stress range, $\Delta\sigma$, (which is synonymous with the applied load range (ΔP)) and the flaw size, or saw-cut length ($2s$). Thus tests were chosen which broke down ΔK_i into its simpler components, varying either ΔP or $2s$. Glass fibre reinforced panels were fatigued with constant saw-cut size but increasing values of ΔP . This resulted in the sequence of separate curves shown in Fig. 4. Carbon fibre reinforced panels were tested at equal values of ΔP , but with different saw-cut lengths (Fig. 5), in this case all the curves converged onto a single curve.

The response of fibre-metal laminates to load ratios ($R = \sigma_{\min}/\sigma_{\max}$) of 0.1 and 0.4 was compared, with

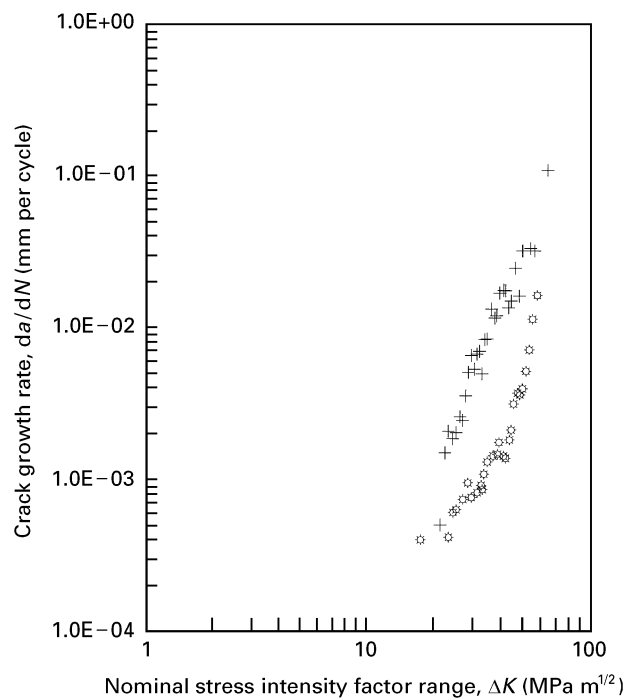


Figure 3 Response of glass fibre reinforced laminates to equal ΔK conditions, Key: (+) 8G3/2; $\Delta K = 16.00 \text{ MPa m}^{1/2}$, $2s = 12 \text{ mm}$; (\odot) 8G3/13; $\Delta K = 16.00 \text{ MPa m}^{1/2}$, $2s = 10 \text{ mm}$.

$\Delta K_i = 8.00 \text{ MPa m}^{1/2}$ and $2s = 10.00 \text{ mm}$ being kept constant. Carbon and glass fibre reinforced laminates were tested (Figs 6 and 7) along with monolithic 8090 (Fig. 8). In all cases the crack growth rates increased with R -ratio without significant differences in curve shape between the three materials.

Reversed loading was used to assess the effect of compressive loads on the bridging mechanism. The panels were clamped between anti-buckling plates and

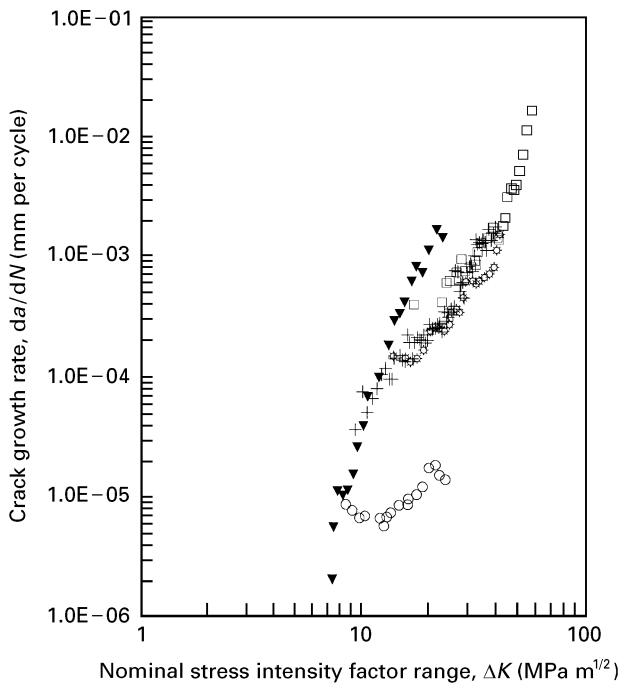


Figure 4 Response of glass fibre reinforced laminates to increasing ΔP , saw-cut length ($2s$) constant. Key: (+) 8G3/1; $\Delta P = 12.24$ kN, (\otimes) 8G3/12; $\Delta P = 15.86$ kN, (\square) 8G3/13; $\Delta P = 19.67$ kN, (\blacktriangledown) 8M1/5, (\circ) 8G3/7; $\Delta P = 10.01$ kN.

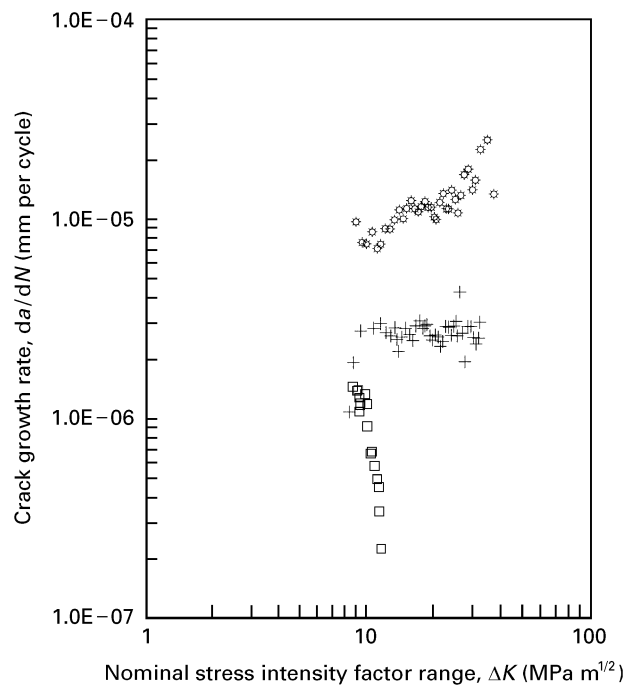


Figure 6 Response of carbon reinforced laminates to changing load ratio and reversed loading. Key: (+) 8C3/15, $R = 0.1$, (\otimes) 8C3/18, $R = 0.4$, (\square) 8C3/6, $R = -0.2$.

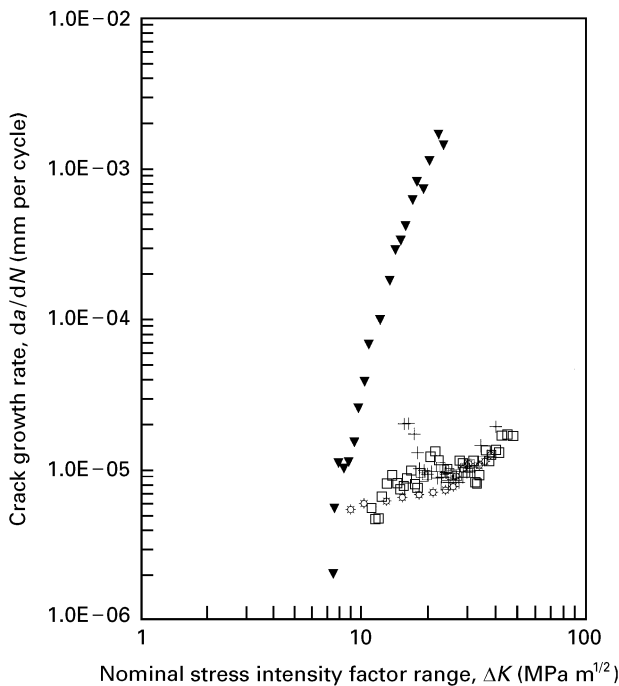


Figure 5 Response of carbon fibre reinforced laminates to increasing $2s$, ΔP constant. Key: (+) 8C3/5; $2s = 20.16$ mm, (\otimes) 8C3/12; $2s = 8.8$ mm, (\blacktriangledown) 8M1/5 (\square) 8C3/16; $2s = 11.80$ mm.

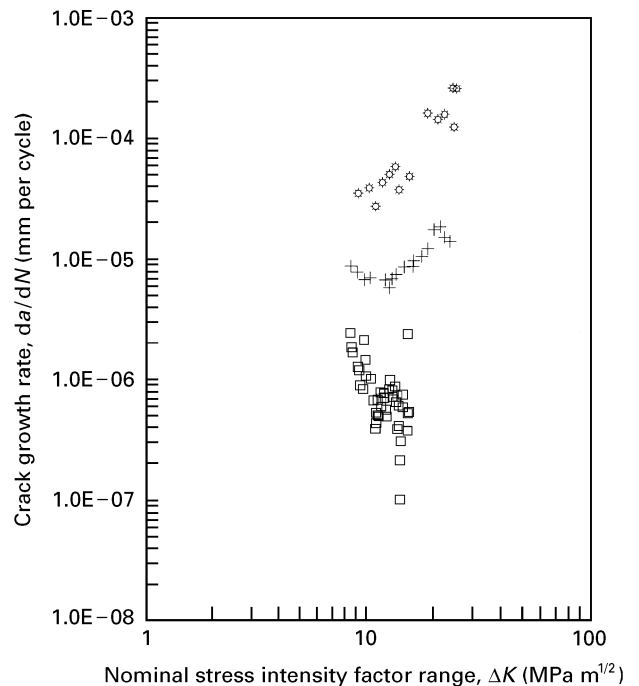


Figure 7 Response of glass reinforced laminates to changing load ratio and reversed loading. Key: (+) 8G3/7; $R = 0.1$, (\otimes) 8G3/5; $R = 0.4$ (\square) 8G3/6; $R = -0.2$.

a loading condition of $R = -0.2$, $\Delta K_i = 7.94$ MPa $m^{1/2}$ and $2s = 10.00$ mm was chosen; this minimized the lateral deflection of the panel beyond the edges of the buckling plates. The applied load range was slightly smaller than that used in the $R = 0.1$ experiments, however the difference is not believed to be significant. Again the tests were carried out on carbon and glass reinforced laminates (Figs 6 and 7) and monolithic

8090 (Fig. 8). The effect of reversed loading on 8090, in terms of the da/dN versus ΔK plot, was to reduce the crack growth rates without significantly changing the shape of the crack growth curve (Fig. 8). The effect of these loading conditions on the laminates was to reduce crack growth rates and drastically change the shape of the crack growth curves, with the cracks in both types of laminate tending to arrest (Figs 6 and 7).

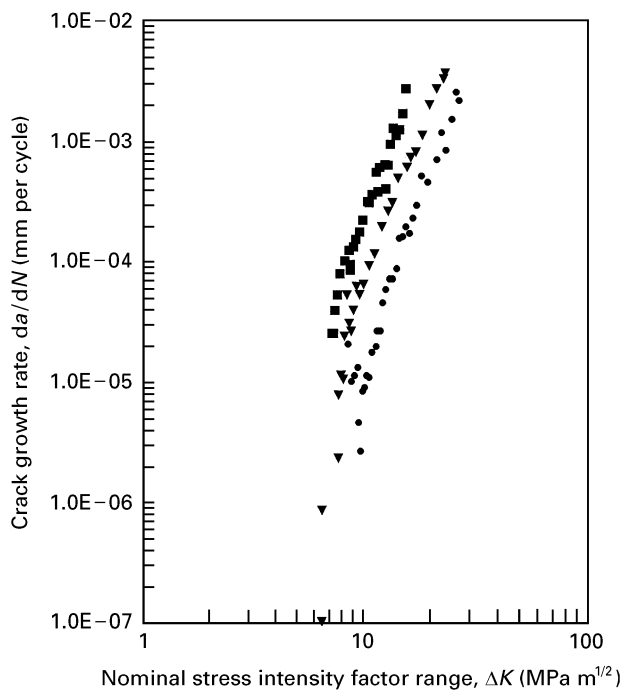


Figure 8 Response of unreinforced 8090 to changing load ratio and reversed loading. Key: (●) 8M1/4, $R = -0.2$, (■) 8M1/2, $R = 0.4$, (▼) 8M1/3, $R = 0.1$.

4. Discussion

4.1. The response of the bridging mechanism

For tests carried out at a constant load ratio monolithic alloys exhibit a unique relationship between crack growth rate and stress intensity factor range. However fatigue testing fibre–metal laminates at different initial ΔK , and constant R -ratio, resulted in a separate growth curve for each test (Fig. 1). Examination of the fatigue crack surfaces from the metal layers of a laminate and from an unreinforced alloy showed that the crack growth process is metallurgically the same in both cases. The crack growth rate remains a function of the ΔK experienced by the crack tip (ΔK_{tip}), but this is no longer equal to the applied ΔK ($\Delta K_{\text{applied}}$) which is calculated from the global parameters of the length of the crack in the metal, the applied stress range and the panel dimensions. Therefore the difference in fatigue response between the two materials must be a function of the response of the fibre bridging mechanism which is a feature of this type of laminate. This can be described by the equations:

$$\frac{da}{dN} = \Delta K_{\text{tip}} \quad (1)$$

$$\Delta K_{\text{tip}} = \Delta K_{\text{applied}} - \Delta K_{\text{bridging}} \quad (2)$$

where $\Delta K_{\text{bridging}}$ is the effective reduction in ΔK caused by the bridging process, following Ritchie *et al.* [2].

Figs 1–3 show that the laminates can exhibit different crack growth rates at the same $\Delta K_{\text{applied}}$, hence $\Delta K_{\text{bridging}}$ must be different in each case. Thus $\Delta K_{\text{bridging}}$ is dependent on the initial load conditions. When discussing fibre–metal laminates not only is the position of the crack growth curve on the da/dN

versus ΔK axes important, but the shape of the curve is also a function of the development of the bridging process with crack length, and merits some attention. Fig. 3 shows two panels fatigued at the same initial ΔK (ΔK_i), yet exhibiting separate growth curves. Notably the shapes of the two curves are dissimilar, revealing that the magnitude and the development of the bridging is not simply dependent on the initial ΔK . This is reinforced by the comparison between two laminates tested at different ΔK_i values (Fig. 2). The panel tested at a higher ΔK_i grew at a lower crack growth rate.

If the curves in Fig. 4 are compared at a single value of $\Delta K_{\text{applied}}$ we can see that the panel tested at a lower ΔP value has a much lower crack growth curve, implying that the magnitude of the bridging effect is much larger therefore bridging is inversely related to ΔP . At the start of each experiment, as shown in Fig. 5, the fatigue crack is not long enough for fibre bridging to be significant and the value of ΔK_i will be representative of the conditions at the crack tip; hence the curves start from different points on the da/dN versus ΔK graph. As the crack grows, and bridging becomes effective, the data rapidly converge onto a single curve. It is believed that this single curve is characteristic of the applied load range.

The relative magnitude of $\Delta K_{\text{bridging}}$ is dependent on, and inversely related to, the applied load range. This explains the behaviour seen in Figs 2 and 3: in both cases the panels were tested under different load ranges, and the panel tested at the lower ΔP exhibited the lower crack growth rates.

Vogelansang *et al.* [1] and Marissen [3] have suggested that the mechanism of delamination growth maintains a constant stress in the fibres. It can be inferred that this stress level is equal for specimens subjected to different load ranges [4]. Consequently the stresses acting on the crack faces to resist crack face opening, and therefore $\Delta K_{\text{bridging}}$, will be constant despite increasing ΔP . This is consistent with the observed results: as ΔP decreases, $\Delta K_{\text{applied}}$ decreases and $\Delta K_{\text{bridging}}$ becomes proportionally larger. In addition $\Delta K_{\text{bridging}}$ would develop more rapidly with respect to $\Delta K_{\text{applied}}$ with lower applied ΔP values, leading to different curve shapes.

4.2. Load ratio (R) effects

In monolithic alloys the increase in crack growth rate with load ratio is commonly associated with a reduction in crack closure effects and this will be operative in both the unreinforced 8090 and the 8090 layers in the laminate.

The ΔP dependence noted earlier indicates that since ΔP was held constant, the relative magnitude of the bridging effect should also remain constant. The delamination zones in the laminates tested at $R = 0.1$ and 0.4 are approximately the same size, implying that the change in R -ratio did not affect the bridging mechanism. It is possible to use Equation 2 to obtain a quantitative estimate of $\Delta K_{\text{bridging}}$. Since the process of crack growth is metallurgically the same for

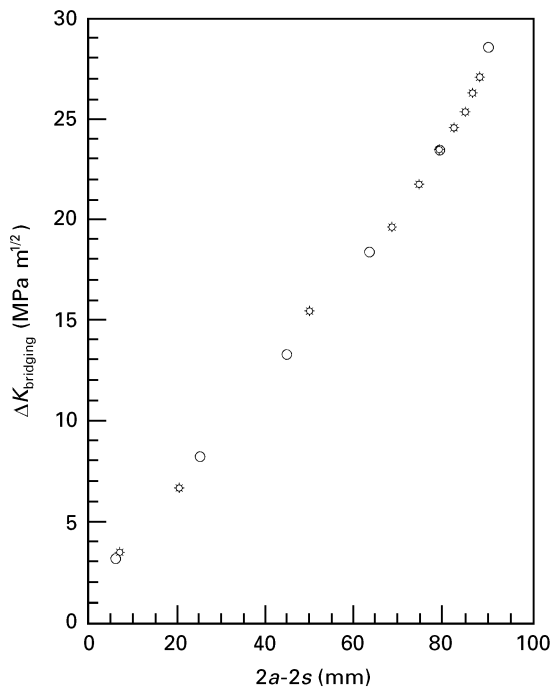


Figure 9 Magnitude of bridging effect for carbon reinforced laminate subjected to $R = 0.1$ and 0.4 Key: (☆) 8C3/18, $R = 0.4$, (○) 8C3/15, $R = 0.1$.

both unreinforced alloys and the metal layers of the laminates, the ΔK at the crack tips must be the same if the cracks in the materials are growing at the same rate when tested under the same R -ratio conditions. Thus, on a da/dN versus ΔK plot, the displacement between points of equal da/dN on the monolithic and laminate growth curves is equal to the magnitude of $\Delta K_{\text{bridging}}$. The magnitude of $\Delta K_{\text{bridging}}$ calculated for the carbon reinforced laminates (Fig. 9) shows that the bridging was unaffected by the change in R -ratio—the ΔP dependence does describe this behaviour.

4.3. Reversed loading effects

When considering reversed loading it is essential to determine whether fibre failure has occurred. Examination of the fatigued specimens in this present work did not reveal any evidence of fibre failure in the crack wake. The delamination zones in these specimens were much smaller than those for the fully tensile cases. It is thought that, because the zones were small and the fibres effectively clamped by the metal plies, buckling of the fibres, and therefore fibre failure, was prevented. Since the fibres remained intact the ΔP dependence, observed for the fully tensile case, should also be applicable to these tests. However the large reduction in crack growth rates, and change in curve shape implies a change in the magnitude of $\Delta K_{\text{bridging}}$ at constant ΔP .

The stresses in the wake fibres and the growth of the delamination are induced by the opening of the crack faces, but this will only occur if the applied loads are tensile. Thus delamination growth is dependent on the tensile portion of ΔP ($\Delta P_{\text{tensile}}$). Under fully tensile conditions, ΔP and $\Delta P_{\text{tensile}}$ are identical, but under

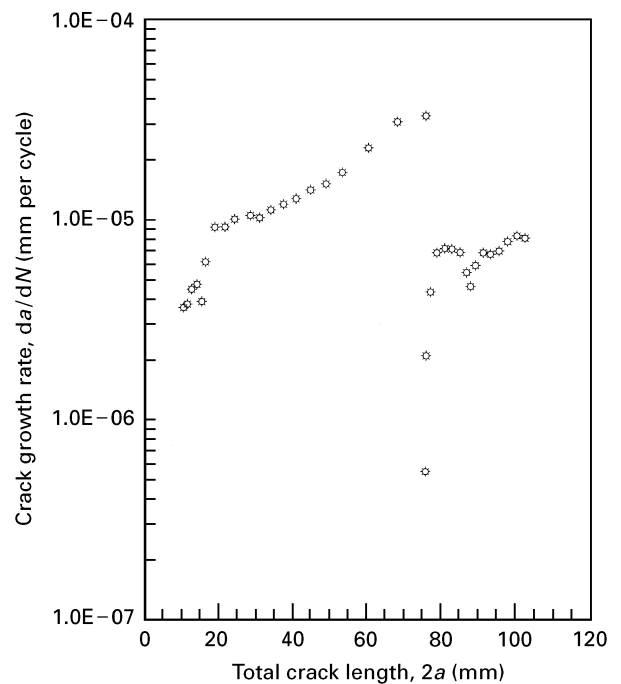


Figure 10 Effect of reversed block load following fully tensile block load on a glass fibre reinforced laminate. Key (☆) 8G3/15.

reversed loading $\Delta P_{\text{tensile}}$ will be much smaller than ΔP , leading to a smaller delamination zone. Thus $\Delta K_{\text{bridging}}$ is inversely related to $\Delta P_{\text{tensile}}$, and if $\Delta P_{\text{tensile}}$ is small, $\Delta K_{\text{bridging}}$ will be relatively large, thus giving the low crack growth rates observed in Figs 6 and 7.

A further test was carried out using two block loads: a fully tensile block until the crack had grown to $2a \approx 70$ mm, followed by a reversed loading condition using the same loads as the tests above (Fig. 10). Although the change to reversed loading resulted in a dramatic reduction in crack growth rate, no crack arrest was observed. It is thought that the crack arrest in the earlier experiments a consequence of the smaller initial flaw size. Crack arrest occurs when $\Delta K_{\text{bridging}}$ is equal to or larger than $\Delta K_{\text{applied}}$. In Fig. 10 the reversed loading was applied after the fatigue crack had grown to ~ 75 mm, under these conditions $\Delta K_{\text{bridging}}$ was no longer greater than $\Delta K_{\text{applied}}$ and crack arrest did not occur.

5. Conclusions

Fibre metal laminates under fatigue loading do not behave in the same manner as unreinforced alloys. The magnitude of the fibre bridging effect depends on the initial loading condition and hence, the dependence of fatigue crack growth rate on initial loading conditions cannot be described simply in terms of ΔK . The crack growth rates depend most strongly on the applied load range, the relative magnitude of the fibre bridging being inversely related to ΔP . This behaviour is thought to be related to the mechanism of delamination growth leading to constant fibre stresses along the crack wake.

In the current work no fibre failure occurred under reversed loading, and in this situation the magnitude of the bridging effect was shown to be inversely related to the tensile portion of the load range, $\Delta P_{\text{tensile}}$. However initial flaw size and prior loading history are believed to be significant factors in the crack growth rate behaviour in these situations.

Acknowledgements

The support of AD Science (Air), Ministry of Defense, together with the technical guidance of DRA Farnborough is gratefully acknowledged.

References

1. L. B. VOGELANG, R. MARISSSEN and J. SCHIJVE, in Proceedings of 11th International Committee on Aeronautical Fatigue (ICAF) Symposium, Noordwijkerhooft, The Netherlands, 20–22 May 1981, 3.4/1.
2. R. O. RITCHIE, WEIKANG YU and R. J. BUCCI, Technical Report UCB/87/AL1049, ALCOA Laboratories, Dec 1987.
3. R. MARISSSEN, Ph.D. thesis, Delft University of Technology, The Netherlands (1988).
4. S. B. DAVENPORT, Ph.D. thesis, University of Southampton, UK (1995).

*Received 17 May
and accepted 2 July 1996*